METTL3-modified lncRNA-MALAT1 regulates the molecular axis of miR-124-3p/CDK4 involved in Ewing's sarcoma

Fangzhou He[1,2], Tingting Ren[1,2], Xiaodong Tang[1,2*]

[1] Department of Musculoskeletal Tumor, People's Hospital, Peking University, 100044, Beijing, China.

[2] Beijing Key Laboratory of Musculoskeletal Tumor, Beijing, China

ARTICLE INFO

ABSTRACT

N6-methyladenosine (m6A) modifications are considered key mechanisms in cancer. As an m6A-modified lncRNA, MALAT1 is associated with tumor progression. In this study, the MALAT1/miR-124-3p/CDK4 axis was studied to discover METTL3's effects on Ewing's sarcoma (ES). For this purpose, clinical ES samples were collected and ES cells were cultured to detect gene expression. Then, the interlink between METTL3, MALAT1, miR-124-3p, and CDK4 was studied and confirmed, and m6A modification of MALAT1 was determined. Finally, the Transwell method was used to test migration and invasion. Results showed that ES samples expressed low miR-124-3p and high METTL3, MALAT1 and CDK4. METTL3 elevated MALAT1 expression by m6A modification. MALAT1 enhanced CDK4 expression by competing with miR-124-3p. In ES cells, METTL3 silencing repressed cell migration and invasion by inhibiting MALAT1. In conclusion, METTL3 promotes tumorigenesis of ES through the MALAT1/miR-124-3p/CDK4 axis.

Introduction

Ewing's sarcoma (ES) mainly occurs in bones or surrounding tissues(1) and is prevalent in children and adolescents, with an incidence of 1/1.5 million(2). According to scientific researches, the age of ES patients mostly ranges from 15 to 20, with males being the susceptible group (3). ES has a high degree of malignancy, a short course, and rapid metastasis. About 30% of patients are accompanied by metastasis to lung, bone, and bone marrow (4)]. At present, the application therapies for ES have unfavorable efficacy (5) and 5-year survival rates in patients with metastatic tumors are reduced to 30%(6). Therefore, in-depth investigations into ES-associated mechanisms are weighty matters to solve the key scientific problems in ES therapy. As an internal mRNA modification, N6-methyladenosine (m6A) modifies gene expression through RNA processing, translation, localization, and degradation (7-8). METTL3-eIF3b interaction modifies gene translation (9) and generates translation complexes in tumors (10). By means of affecting RNA stability, mRNA degradation and translation, METTL3 is essential in the process of gene expression regulation (11). In addition, with the regulative effects in cell differentiation, tissue development, and tumorigenesis, methylation of m6A mRNA initiated by METTL3 is likely to cause diseases as well as tumors among a large number of mammals (12). It has been emphasized that METTL3 can promote tumor growth and metastasis (13), but its biomolecular mechanism in ES still needs to be further explored.METTL3 initiates the methylation of m6A mRNA, which is recognized by proteins containing the YTH domain (14), thus regulating mRNA splicing, stability, and translation(15). Although the function of YTH domains in various organisms has been partially clarified, the mechanism of m6A regulating gene expression in ES remains elusive. Emerging reports have underlined the importance of lncRNAs in normal cell development and physiological functions(16-18). As a conserved 7-9 kbp lncRNA with evolutionary significance, MALAT1 is recognized for its association with tumor progression (19) and METTL3 upregulates MALAT1 at the transcription level by triggering m6A modification (11,18)].In view of the carcinogenic effect of MALAT1, the study prepared an evaluation to test how METTL3-modified MALAT1 in ES functioned biologically through the miR-124-3p/CDK4 axis.

Materials and Methods

Collection of clinical samples

ES tissue and their matched normal tissue were received from patients undergoing surgery and temporarily frozen in liquid nitrogen before preservation at -80°C.

ES cell lines

ES cell lines SK-ES-1, A673, and RD-ES (ATCC, USA) were cultured in DMEM (Corning) with the supplement of 10% FBS (Omega Scientific) and 100 U/100 µg, 2 mM glutamine (Invitrogen, USA).

Cells transfection

Invitrogen took over the design and supplement of all interference and over-expression plasmids (sh-MALAT1, oe-MALAT1, sh-METTL3, miR-124-3p inhibiter, *miR-*

124-3p-mimic, oe-CDK4, and related controls). Lipofectamine 2000 (11,668,019, Thermo Fisher Scientific) was purchased for the transfection of cells. The individual well of the 6-well plate was inoculated with 1×10^5 cells and cultured until the cell confluence reached 60-70%. Then 4 μg plasmid was diluted with 10 μL transfection solution using 250 μL Opti-MEM with no serum (Gibco) and loaded onto the plate. A fresh complete medium was an alternative after 6 h.

Quantitative PCR

Trizol was used to extract total RNA from tissues or cells (Invitrogen), while the analysis was carried out by using Nanodrop2000, the micro-ultraviolet spectrophotometer named (1011U, Nanodrop). Primers were used in the process of reverse transcription in TaqMan MicroRNA Assays (4,427,975, Applied Biosystem). In addition, the reverse transcription into cDNA of PrimeScript RT reagent Kit (RR047A, Takara) has also been realized. TaKaRa was in charge of the design and synthesis of all primers (Table S1). While detecting quantitative PCR, the ABI7500 quantitative PCR instrument (7500, ABI), as well as SYBR Green Rapid PCR Kit (Applied Biosystems) was applied. Reference controls were GAPDH and U6.

Immunoblotting

In tissues and cells, the extraction of total protein was carried out with RIPA lysis buffer which contained PMSF (P0013C, Beyotime, China), while the quantification was realized by using a BCA assay kit (P0012, Beyotime). After being dissolved in $2 \times$ SDS sample buffer, the 50 μg protein sample was boiled for 10 min for SDS-PAGE, before the transfer to the PVDF membrane. After a 1-hour enclosure in 5% skim milk, the membrane was blended with primary antibody (Abcam) overnight: METTL3 (1:1000, ab195352), CDK4 (ab108357, 1:2500) and GAPDH (ab9485 1:2500), and the corresponding secondary antibody for the Durance of one hour: HRP-labeled goat anti-rabbit IgG (ab97051, 1:2000, Abcam). Blots were developed with ECL (BB-3501, Amersham), and imaged in Bio-Rad, a system of image analysis, while the analysis was carried out by using Quantity-One (v4.6.2) software.

Immunohistochemical staining

ES tissues were linked to 10% neutral formalin, followed by dehydration and paraffin embedment. The prepared slices were successively processed with xylene and gradient alcohol for dewaxing and dehydration, respectively and inactivated with 3% H_2O_2. Next, slices were boiled for 30 minutes in 10 mM sodium citrate (pH 6.0) before being sealed for 15 min in 10% normal goat serum prior to overnight incubation with METTL3 (1:500, ab195352, Abcam) or CDK4 1:500, ab108357, Abcam) at 4℃. On the second day, the secondary antibody was reacted for 1 h. Immunohistochemical images were quantitatively analyzed by ImageJ

Transwell assays

Matrigel (YB356234, Umibio, Shanghai, China), stored at -80℃, was removed and left overnight at 4℃ in order to be liquefied, before the dilution of the 200 μL matrigel and the 200 μL serum-free medium. Next, a 50 μL diluted sample was left in the top compartment of each plate for 2-3 h and supplemented with ES cells (2×10^4/ well) for 24 h. Meanwhile, the lower compartment was mixed with an amount of 800 μL medium which contained 20% FBS. Afterward, the Transwell plates were soaked for 10 min in 10% formaldehyde and then rinsed with clean water three times. Next, staining was performed after the 30-min interaction with 0.1% crystal violet (Solarbio, Beijing, China) and observed under a microscope. Matrigel was not necessary for the process of the transwell migration experiment, with a 16-hour culture time.

Methylated RNA immunoprecipitation (MeRIP)

Trizol method was applied to isolate total RNA from cells, while the incubation with protein A/G magnetic beads in IP buffer (20 mM Tris, pH 7.5, 2 mM EDTA, 1% NP-40, and 140 mM NaCl) was carried out in the PolyATtract®mRNA Isolation Systems, which contained anti-m6A (1:500, ab151230, Abcam) or anti-IgG (ab109489, 1:100, Abcam) (A-Z5300, ATECHENGINEE-RING). mRNA-bead complexes were then added after an hour to a RIP buffer which contained ribonuclease inhibitors and protease inhibitors, before overnight incubation at 4℃. The elution and purification of RNA were carried out by using phenol-chloroform to measure MALAT1 expression using the method of quantitative PCR.

Photoactivatable ribonucleoside-enhanced crosslinking immunoprecipitation (PAR-CLIP)

ES cells were added to 200 mM 4-thiopyridine (4SU) (Sigma Aldrich, St. Louis, MO, USA) for 14 hours, and then crosslinked with 0.4 at 365 J/cm2 nanoparticles. The lysate was immunoprecipitation with METTL3 antibody before an overnight incubation at 4 ℃. With the label [g-32P] - ATP, RNA was observed with the assistance of autoradiography. In order to remove protein while detecting the relative quantitative expression of MALAT1, protease K was added to digest the sediment.

Reporter test using dual luciferase

Containing the binding site of miR-124-3p, CDK4-3'UTR and MALAT1 cDNA fragments were inserted into the pGL3 plasmid. The binding site was mutated and the resulting fragments were inserted into the pGL3 plasmid. After gene sequencing, pGL3-MALAT1, pGL3-MALAT1-MUT, pGL3-CDK4-3'UTR, and pGL3-CDK4-3'UTR-MUT were transfected with miR-124-3p mimic or NC-mimic, respectively into the cells of HEK-293. Cell lysis was collected after 48 h and loaded onto a gene analysis system using dual luciferase (Promega) which is based on Luciferase Assay Kit (K801-200, Biovision) [25].

Ago2 RIP

RIP kits (Millipore) were purchased for RIP assays. Cells were dissolved for 30 min in an equal volume of RIPA lysis buffer (p0013B, Beyotime), the supernatant was obtained at 4℃ after centrifugation at 14000 rpm for durance of 10 minutes. With about 50 μL magnetic beads added into the co-precipitation system and resuscitated in 100 μL RIP washing buffer, 5 μg rabbit anti-AGO2 (ab186733, 1:50, Abcam) or rabbit IgG (ab172730, 1:100, Abcam) was then mixed at a temperature of 4℃ for no less than 6 hours. After buffer washing, the re-suspension of the antibody complex was realized with 900 μL RIP washing buffer, while RNA was extracted for quantitative

PCR after the digestion of protease K.

Statistical analysis

All data are expressed as mean ± standard deviation. The analysis involved was carried out by using SPSS 24.0 software and compared by paired or unpaired t-tests, respectively. The Tukey test was used in the one-way ANOVA so as to compare the related multiple groups. It is worth mentioning that $P < 0.05$ was essential in the aspect of statistics.

Results

METTL3 induces m6A RNA methylation of MALAT1

METTL3 and MALAT1 levels were examined in ES. As tested, METTL3 and MALAT1 were upregulated in ES (Figure 1A, B). METTL3 was silenced with sh-METTL3 in ES cells (Figure 1C, D). Then, Me-RIP analyzed that m6A RNA methylation of MALAT1 was suppressed after silencing METTL3 (Figure 1E). Furthermore, PAR-CLIP
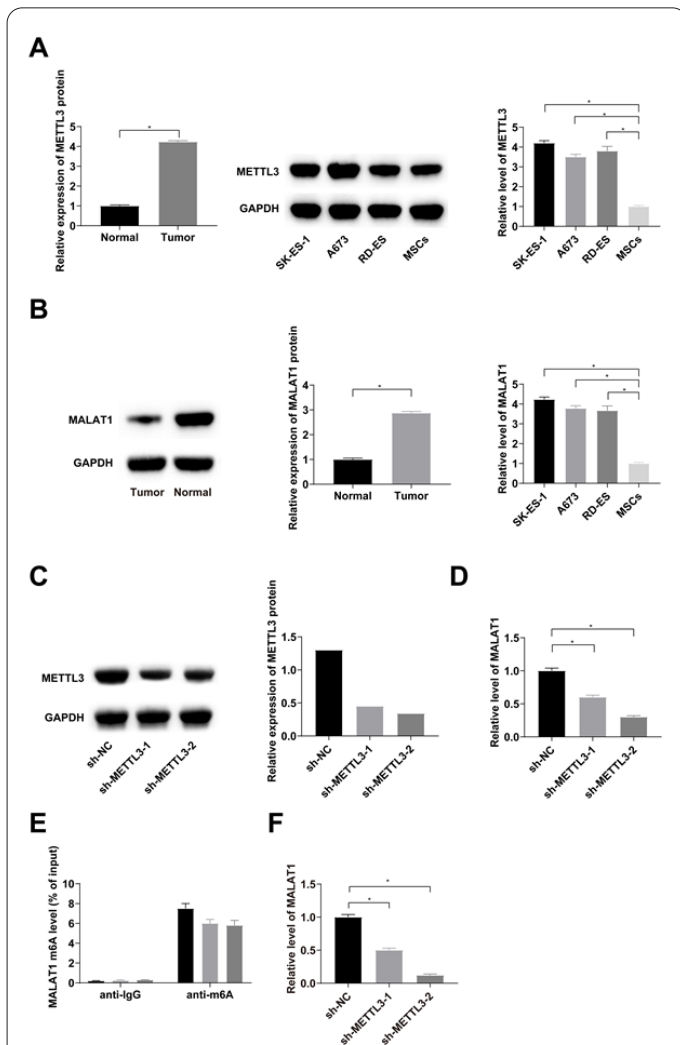
Figure 1. METTL3 upregulates MALAT1 by m6A RNA methylation of MALAT1. A: Immunoblotting and immunohistochemical detection of METTL3 expression in ES tissues and qRT-PCR detection of METTL3 in ES cells., B: Immunoblotting and immunohistochemical detection of MALAT1 in ES tissues and qRT-PCR detection of MALAT1 expression in ES cells. C: Immunoblotting tested METTL3 after METTL3 silencing. D: Quantitative PCR measured MALAT1 expression after METTL3 silencing. E: Me-RIP analyzed the level of MALAT1 in the process of m6A RNA methylation after METTL3 silencing. F: PAR-CLIP detected METTL3 and MALAT1 binding.

detected the reduced interaction between METTL3 and MALAT1 after METTL3 silencing (Figure 1F).

METTL3 silencing prevents ES cells from migrating and invading by inhibiting MALAT1

SK-ES-1 cells became the objects in the following cellular experiments. Following sh-NC transfection, oe-MALAT1 caused no change in METTL3 expression, but elevated MALAT1 expression. sh-METTL3 transfection reduced both METTL3 and MALAT1 expression, but follow-up oe-MALAT1 treatment recovered MALAT1 expression (Figure 2A, B). Transwell detection results demonstrated that overexpressing MALAT1 enhanced the migratory and invasive ability of ES cells, but silencing METTL3 had the opposite effect. Functionally, MALAT1 upregulation weakened the anti-migration/invasion effect of silencing METTL3 (Figure 2C-D).

A proven binding between MALAT1 and miR-124-3p

In StarBase (http://starbase.sysu.edu.cn/index.php), the relative researches have proved the sequences of binding between MALAT1 and miR-124-3p (Figure 3A). To estimate the regulatory effect of MALAT1 on miR-124-3p, the expression of the latter was measured in ES which turned out to be in a low state (Figure 3B, C). Next, in MALAT1-silenced ES cells, miR-124-3p expression increased (Figure 3D, E). Next, through luciferase reporter gene assay, the discovery has been made that miR-124-3p mimic had a limited reductive effect only on the luciferase activity of pGL3-MALAT1 (Figure 3F). In the meanwhile, the results of RIP manifested that MALAT1 was enriched with miR-124-3p in Ago2 (Figure 3G).
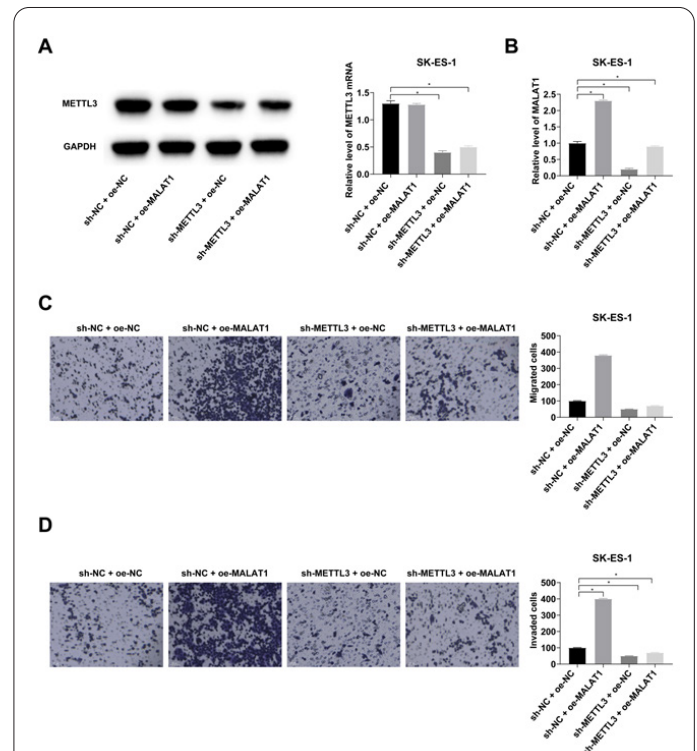
Figure 2. With the inhibitive effects on MALAT1 expression, METTL3 silencing can impede migration and invasion in ES cells. A: Immunoblotting tested METTL3 protein. B: Quantitative PCR measured MALAT1. C-D: Transwell method determined cell migration and invasion.
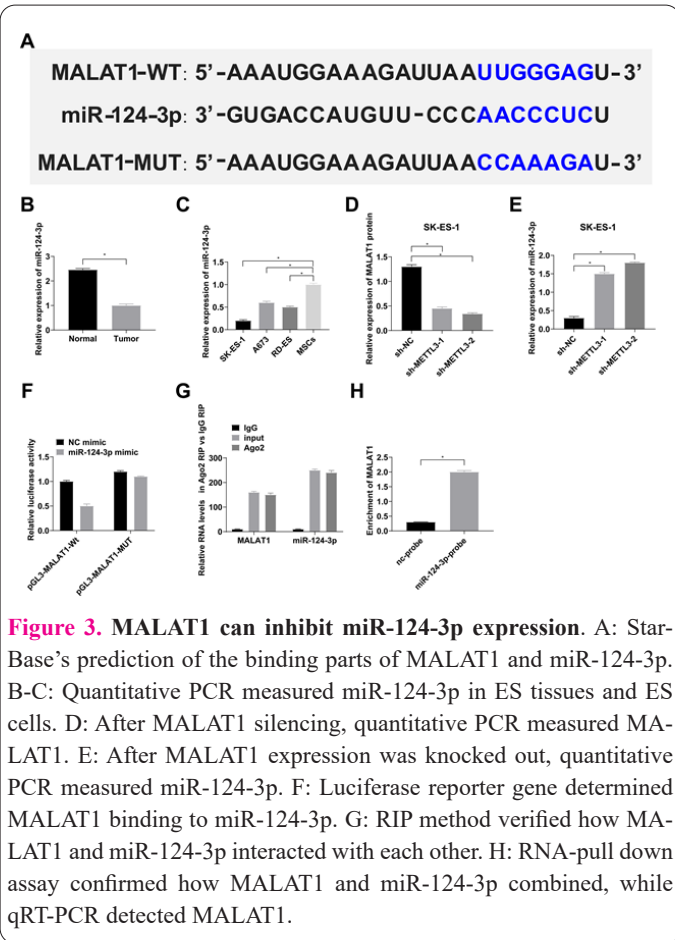
Figure 3. MALAT1 can inhibit miR-124-3p expression. A: Star-Base's prediction of the binding parts of MALAT1 and miR-124-3p. B-C: Quantitative PCR measured miR-124-3p in ES tissues and ES cells. D: After MALAT1 silencing, quantitative PCR measured MA-LAT1. E: After MALAT1 expression was knocked out, quantitative PCR measured miR-124-3p. F: Luciferase reporter gene determined MALAT1 binding to miR-124-3p. G: RIP method verified how MA-LAT1 and miR-124-3p interacted with each other. H: RNA-pull down assay confirmed how MALAT1 and miR-124-3p combined, while qRT-PCR detected MALAT1.

Figure 4. MALAT1 can promote CDK4 expression by competing with miR-124-3p. A: StarBase's prediction of binding parts between CDK4 and miR-124-3p. B: Immunoblotting and Quantitative PCR detected CDK4 in ES tissues. C: Quantitative PCR measured CDK4 in ES cells. D: Luc confirmed the binding of miR-124-3p to CDK4. E: Quantitative PCR measured miR-124-3p. F: quantitative PCR measured CDK4 expression.

MALAT1 can promote CDK4 expression through competing with miR-124-3p

miR-124-3p shared binding sites in CDK4 3'UTR in Starbase database (Figure 4A). CDK4 in tumor tissues was detected by immunoblotting and immunohistochemistry. Interestingly, CDK4 expression in ES was elevated (Figure 4B, C). Referring to the results of luciferase reporter gene detection, the miR-124-3p mimic had an inhibitive effect on the luciferase activity of pGL3-miR-124-3p-3'UTR (Figure 4D). Next, to study further how miR-124-3p regulated CDK4, miR-124-3p was expressed overly and then successfully silenced in ES cells (Figure 4E). Responded to miR-124-3p over-expression, ES cells expressed CDK4 in an inhibited stage, while ES cells had higher CDK4 expression when miR-124-3p was downregulated (Figure 4F).

MALAT1 triggers the migration and invasion of ES cells through miR-124-3p-controlled CDK4 expression

When exploring the functional role of MALAT1 in ES cells by targeting miR-124-3p/CDK4, the study found that sh-MALAT1 lowered CDK4 expression, which was however recovered by miR-124-3p inhibiter. The reduced expression of CDK4, which was controlled by miR-124-3p, was rescued after interference with oe-CDK4 (Figure 5A). Transwell assay results determined that miR-124-3p inhibitor abolished sh-MALAT1-induced suppression of ES cell migration; the anti-migratory ability of miR-124-3p mimic was rescued by oe-CDK4 (Figure 5B, C).

Discussion

The indispensable and diversified role of lncRNAs in human cancer has aroused great interest of more and
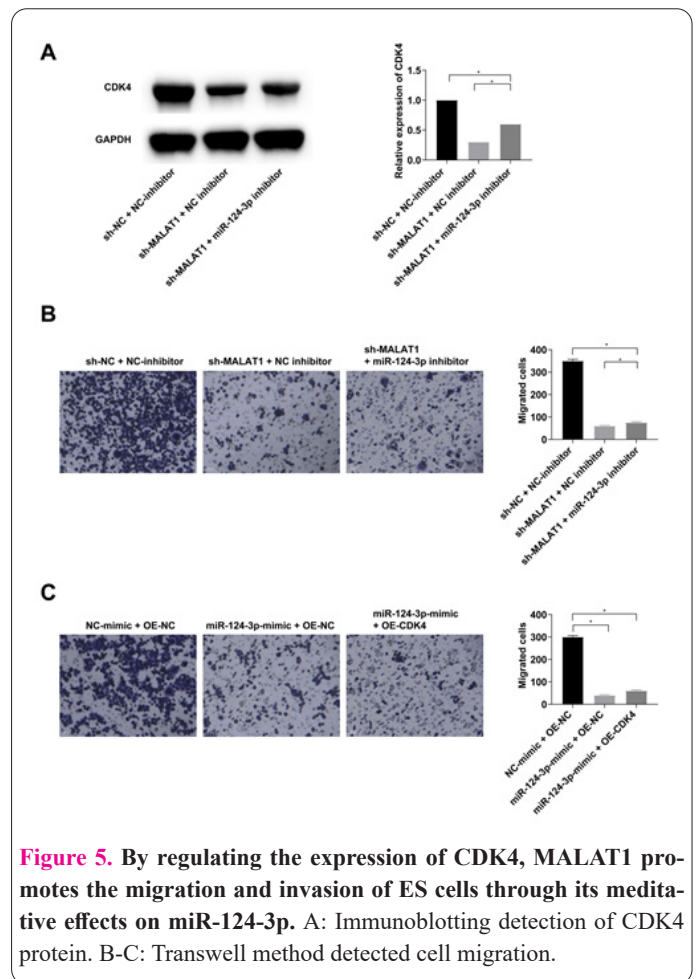
Figure 5. By regulating the expression of CDK4, MALAT1 promotes the migration and invasion of ES cells through its mediative effects on miR-124-3p. A: Immunoblotting detection of CDK4 protein. B-C: Transwell method detected cell migration.

more researchers' attention (20) with the discovery of new lncRNAs by sequencing technologies (21). On this basis, bioinformatics tools have helped researchers discover deep interactions between lncRNAs and human cancer (22).

In ES, MALAT1 was found to be upregulated, suggesting oncogenic pathogenesis in the disease. Previously, a report on colorectal cancer has determined aberrant high expression of MALAT1 and further supported its tumor-promoting effect regarding epithelial-mesenchymal transformation and angiogenesis through competing with miR-126-5p (23). Moreover, MALAT1 is related to inva-

siveness in the microenvironment of ovarian cancer (19) and breast cancer (24). In short, MALAT1 may act as a carcinogenic agent in ES.

Interestingly, MALAT1 can mediate miRNA expression through an absorption mechanism (25). The study speculated that a similar regulatory mechanism may also exist in ES and eventually determined how MALAT1 was linked to miR-124-3p. In ES, according to the relative illustrations, the dependent role of the CDK4/6 pathway has been proved (26). Therefore, the study identified a specific single-agent inhibitor target (CDK4/6) and found the binding relationship of miR-124-3p to CDK4, which has been studied previously (27). Considering ES patients' prognosis, CDK4 high expression is an unfavorable index (28-29). Mechanistically, our analysis of ES cells confirmed that METTL3-modified MALAT1 could mediate CDK4 expression through miR-124-3p, thus triggering ES cells to migrate and invade.

However, it is still unclear how METTL3 controls MALAT1 expression in ES. Given the characteristics of METTL3-mediated m6A modification of MALAT1, further studies are warranted to identify specific effector factors involved in m6A modifications that regulate MALAT1 expression levels.

METTL3 regulates the migration and invasion of ES cells through the MALAT1/miR-124-3p/CDK4 axis, constructing a cascade of regulatory mechanisms. Our study initially focuses on the METTL3/MALAT1/miR-124-3p/CDK4 axis in ES and further elaborates on METTL3-mediated m6A modification in ES.

References

1. Pinto A, Dickman P, Parham D. Pathobiologic markers of the ewing sarcoma family of tumors: state of the art and prediction of behaviour. Sarcoma. 2011;2011:856190.

2. Ross, K.A., et al., The biology of ewing sarcoma. ISRN Oncol 2013. 2013: p. 759725.

3. Khan S, Abid Z, Haider G, et al. Incidence of Ewing's Sarcoma in Different Age Groups, Their Associated Features, and Its Correlation With Primary Care Interval. Cureus 2021;13(3):e13986.

4. Aghighi M, Boe J, Rosenberg J, et al. Three-dimensional Radiologic Assessment of Chemotherapy Response in Ewing Sarcoma Can Be Used to Predict Clinical Outcome. Radiol 2016;280(3):905-15.

5. Ludwig JA, Meyers PA, Dirksen U. Ewing's Sarcoma. N Engl J Med. 2021;384(15):1476.

6. Barrett C, Budhiraja A, Parashar V, et al. The Landscape of Regulatory Noncoding RNAs in Ewing's Sarcoma. Biomed 2021;9(8):933.

7. Wang CX, Cui GS, Liu X, et al. METTL3-mediated m6A modification is required for cerebellar development. PLoS Biol 2018;16(6):e2004880.

8. Roundtree IA, Evans ME, Pan T, et al. Dynamic RNA Modifications in Gene Expression Regulation. Cell 20175;169(7):1187-1200.

9. Lin S, Choe J, Du P, et al. The m(6)A Methyltransferase METTL3 Promotes Translation in Human Cancer Cells. Mol Cell 2016;62(3):335-345.

10. Yang Y, Fan X, Mao M, et al. Extensive translation of circular RNAs driven by N6-methyladenosine. Cell Res 2017;27(5):626-641.

11. Jin D, Guo J, Wu Y, et al. m6A mRNA methylation initiated by METTL3 directly promotes YAP translation and increases YAP

12. Pan Y, Ma P, Liu Y, et al. Multiple functions of m6A RNA methylation in cancer. J Hematol Oncol 2018;11(1):48.

13. Li T, Hu PS, Zuo Z, et al. METTL3 facilitates tumor progression via an m6A-IGF2BP2-dependent mechanism in colorectal carcinoma. Mol Cancer 2019;18(1):112.

14. Gao Y, Pei G, Li D,et al. Multivalent m6A motifs promote phase separation of YTHDF proteins. Cell Res 2019;29(9):767-769.

15. Xu C, Wang X, Liu K, et al. Structural basis for selective binding of m6A RNA by the YTHDC1 YTH domain. Nat Chem Biol 2014;10(11):927-9.

16. Lorenzi L, Avila Cobos F, Decock A, et al. Long noncoding RNA expression profiling in cancer: Challenges and opportunities. Genes Chromosomes Cancer. 2019;58(4):191-199.

17. Pillay S, Takahashi H, Carninci P, et al. Antisense RNAs during early vertebrate development are divided in groups with distinct features. Genome Res 2021;31(6):995-1010.

18. Zhao C, Ling X, Xia Y, et al. The m6A methyltransferase METTL3 controls epithelial-mesenchymal transition, migration and invasion of breast cancer through the MALAT1/miR-26b/HMGA2 axis. Cancer Cell Int 2021 ;21(1):441.

19. Mao TL, Fan MH, Dlamini N, et al. LncRNA MALAT1 Facilitates Ovarian Cancer Progression through Promoting Chemoresistance and Invasiveness in the Tumor Microenvironment. Int J Mol Sci 2021;22(19):10201.

20. Yu Y, Zhang M, Liu J, et al. Long Non-coding RNA PVT1 Promotes Cell Proliferation and Migration by Silencing ANGPTL4 Expression in Cholangiocarcinoma. Mol Ther Nucleic Acids 2018;13:503-513.

21. Liu B, Wu S, Ma J, Yan S, Xiao Z, Wan L, Zhang F, Shang M, Mao A. lncRNA GAS5 Reverses EMT and Tumor Stem Cell-Mediated Gemcitabine Resistance and Metastasis by Targeting miR-221/SOCS3 in Pancreatic Cancer. Mol Ther Nucleic Acids 2018 Dec 7;13:472-482.

22. Wu J, Qi X, Liu L, et al. Emerging Epigenetic Regulation of Circular RNAs in Human Cancer. Mol Ther Nucleic Acids 2019;16:589-596.

23. Sun Z, Ou C, Liu J, et al. YAP1-induced MALAT1 promotes epithelial-mesenchymal transition and angiogenesis by sponging miR-126-5p in colorectal cancer. Oncogene. 2019r;38(14):2627-2644.

24. Wang N, Cao S, Wang X, et al. lncRNA MALAT1/miR26a/26b/ST8SIA4 axis mediates cell invasion and migration in breast cancer cell lines. Oncol Rep 2021;46(2):181.

25. Dai X, Chen C, Xue J, et al. Exosomal MALAT1 derived from hepatic cells is involved in the activation of hepatic stellate cells via miRNA-26b in fibrosis induced by arsenite. Toxicol Lett 2019;316:73-84.

26. Guenther LM, Dharia NV, Ross L, et al. A Combination CDK4/6 and IGF1R Inhibitor Strategy for Ewing Sarcoma. Clin Cancer Res 2019;25(4):1343-1357.

27. Cassier P, Pissaloux D, Alberti L, et al. Traitements ciblés des sarcomes et des tumeurs conjonctives rares [Targeted treatment of rare connective tissue tumors and sarcomas]. Bull Cancer 2010;97(6):693-700.

28. Kennedy AL, Vallurupalli M, Chen L, et al. Functional, chemical genomic, and super-enhancer screening identify sensitivity to cyclin D1/CDK4 pathway inhibition in Ewing sarcoma. Oncotarget 2015;6(30):30178-93.

29. Lei X, Yang S, Yang Y, et al. Long noncoding RNA DLX6-AS1 targets miR-124-3p/CDK4 to accelerate Ewing's sarcoma. Am J Transl Res 2019;11(10):6569-6576.